Nickel Nanocatalyst Hot Paper

How to cite: *Angew. Chem. Int. Ed.* **2021**, *60*, 18591 – 18598
International Edition: doi.org/10.1002/anie.202105492
German Edition: doi.org/10.1002/ange.202105492

Ambient Hydrogenation and Deuteration of Alkenes Using a Nanostructured Ni-Core–Shell Catalyst

Jie Gao, Rui Ma, Lu Feng, Yuefeng Liu, Ralf Jackstell, Rajenahally V. Jagadeesh, and Matthias Beller**

In memory of Professor Paul C. J. Kamer

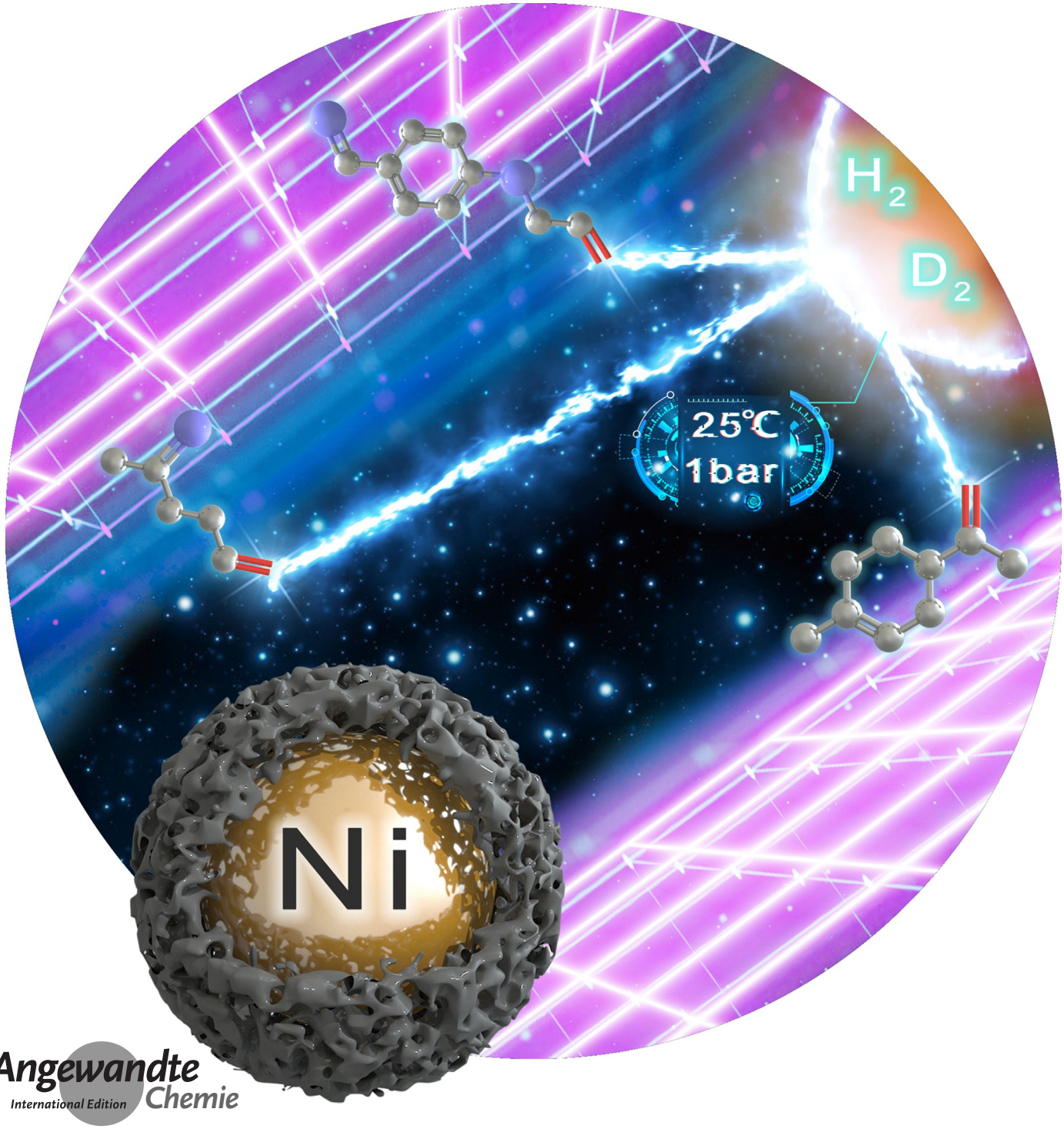

Abstract: *A general protocol for the selective hydrogenation and deuteration of a variety of alkenes is presented. Key to success for these reactions is the use of a specific nickel-graphitic shell-based core–shell-structured catalyst, which is conveniently prepared by impregnation and subsequent calcination of nickel nitrate on carbon at 450 °C under argon. Applying this nanostructured catalyst, both terminal and internal alkenes, which are of industrial and commercial importance, were selectively hydrogenated and deuterated at ambient conditions (room temperature, using 1 bar hydrogen or 1 bar deuterium), giving access to the corresponding alkanes and deuterium-labeled alkanes in good to excellent yields. The synthetic utility and practicability of this Ni-based hydrogenation protocol is demonstrated by gram-scale reactions as well as efficient catalyst recycling experiments.*

Introduction

Alkenes serve as key feedstocks and central intermediates in chemical, pharmaceutical, petrochemical, and material industries. Indeed, a variety of bulk and fine chemicals as well as renewables contain C=C double bonds. Although the majority of these products are used for further alkene polymerization[1] or functionalizations to give ketones,[2] alcohols,[3] epoxides,[4] and amines,[5] the apparently simple hydrogenation to give alkanes is also important.[6–11] Specifically, in the petrochemical industry hydrotreating of petroleum and its derivatives is applied on large scale.[12] Another prominent industrial process is the conversion of diisobutene mixtures to isooctane (2,4,4-trimethylpentane), an important component of gasoline, commonly used to increase the knock resistance of fuels. In addition, the selective hydrogenation of bio-feedstocks, such as 2-methoxy-4-allylphenol (eugenol), (+)-limonene, and related terpenes, is gaining increasing attention for producing renewable fine chemicals, for example, fragrances.[13,14]

With respect to fine chemicals, catalytic hydrogenations are used in the synthesis of vitamins such as biotin, a vitamin K3 derivative, and β-carotene. Moreover, olefin hydrogenation processes are applied for the conversion of natural unsaturated oils to processable and storable fats on multi-million-ton scales for the food industries.[15,16] Typically, these reductions rely on Raney nickel® or the palladium-based Lindlar catalyst. Unfortunately, both materials have certain disadvantages: While the former is highly sensitive and requires special handling, the latter is quite expensive. In addition, the majority of these reactions require high pressure of hydrogen (up to 50 bar) and sometimes higher reaction temperatures (> 100 °C), which requires specific equipment and additional energy.[11,17] In this respect, the development of more active catalysts which allow for minimal energy consumption and low pressure is highly desired, but scientifically very challenging. So far, such hydrogenations can only be achieved under mild conditions in the presence of precious metal catalysts. However, at this point it should also be noted that due to the exothermicity of hydrogenations for large scale applications low temperature reactions are not ideal because such processes would require cooling. Thus, hydrogenations at ambient conditions specifically offer advantages for fine chemical products and organic synthesis. Apart from that, a modern state-of-the-art catalyst for olefin hydrogenation should be based on 3d-metals due to their availability and price advantages.

Notably, in recent years important breakthroughs were reported for the hydrogenation of alkenes in the presence of homogeneous Fe-, Co-, and Ni-based complexes.[6,18,19] For example, bis(NHSi) Ni complexes,[6] cobalt dihydrogen complexes,[19] and iron dinitrogen complexes[18] can be successfully applied under mild conditions. However, these homogeneous complexes are rather sensitive and/or require sophisticated synthetically demanding ligands, which makes them less feasible for practical hydrogenations of alkenes. On the other hand, heterogeneous catalysts are generally more stable and permit easier recycling and reusability.[20–28] In this respect, we recently introduced nanostructured materials based on the pyrolysis of cobalt salts and biopolymers for the hydrogenation of alkenes, however these materials also showed no hydrogenation reactivity at ambient conditions.[11,17] In fact, to the best of our knowledge, until now 3d-metal-based heterogeneous catalysts for the hydrogenation of alkenes at ambient conditions (1 bar hydrogen, RT) have not been reported.

Here, we report the preparation of novel core–shell Ni-nanoparticles supported on Vulcan XC72R by impregnation and subsequent calcination. The resulting materials exhibit excellent activity for the selective hydrogenation and deuteration of terminal and internal alkenes including functionalized ones under very mild conditions.

Results and Discussion

Catalyst Preparation and Initial Testing

To prepare highly active supported 3d-metal nanoparticles for olefin hydrogenation, several metal nitrates (Fe, Mn, Co, or Ni) were impregnated in MeOH on carbon (Vulcan XC72R), Al_2O_3, V_2O_5, CeO_2, TiO_2, and C_3N_4. Upon slow evaporation of the solvent the corresponding metal nitrates were adsorbed onto the support. The resulting materials were

[*] J. Gao, R. Ma, Dr. R. Jackstell, Dr. R. V. Jagadeesh, Prof. Dr. M. Beller
Leibniz Leibniz-Institut für Katalyse e.V.
Albert-Einstein-Strasse 29a, 18059 Rostock (Germany)
E-mail: jagadeesh.rajenahally@catalysis.de
matthias.beller@catalysis.de
L. Feng, Dr. Y. Liu
Dalian National Laboratory for Clean Energy (DNL)
Dalian Institute of Chemical Physics
Chinese Academy of Science
457 Zhongshan Road, 116023 Dalian (China)
Supporting information and the ORCID identification number(s) for the author(s) of this article can be found under: https://doi.org/10.1002/anie.202105492.

calcined under argon at defined temperatures (350–750 °C) to obtain a small library of potential catalysts (Figure 1). Hereafter, we represent these supported nanoparticles as M@support-X, where M and X denote the metal and pyrolysis temperature, respectively.

Figure 1. General preparation of supported 3d-metal-based catalysts.

Initial catalytic experiments were carried out for the hydrogenation of 1-decene as a benchmark reaction under challenging reaction conditions (room temperature and 1 bar hydrogen in methanol). As expected, all homogeneous metal salts and their supported congeners were completely inactive under these reaction conditions (Table S1). Next, we tested calcined materials, e.g., Fe@C-450, Cu@C-450, Co@C-450, and Ni@C-450. None of the Fe-, Cu-, and Co-based materials showed any activity (Table 1, entries 1–3), instead the Ni-based catalyst (Ni@C-450) exhibited excellent activity and 1-decene was reduced to *n*-decane in quantitative yield (Table 1, entry 4).

To understand the effect of calcination temperature, Ni@C was calcined at different temperatures (350–750 °C). Among these, only Ni@C-450 and Ni@C-550 were found to be active (Table 1, entries 5–8). In addition, the influence of supports was also evaluated. For this purpose, Ni-nitrate was impregnated on Al_2O_3, V_2O_5, CeO_2, TiO_2, and C_3N_4 and calcined at 450 °C under argon. However, all these materials were completely inactive (Table S1). Next, the performance of Ni@C-450 in other solvents such as toluene, acetonitrile, ether, tetrahydrofuran, and 2-propanol was assessed (Table S2). Compared to methanol, all other solvents showed poor catalyst activity. As a control experiment, the reaction in the absence of hydrogen revealed no conversion of alkene, which confirms H_2 as the sole reducing agent and no transfer hydrogenation mechanism (Table S2).

Table 1: Hydrogenation of 1-decene using different catalysts under ambient conditions.

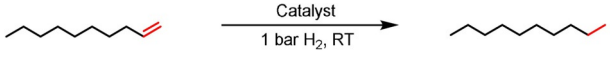

Entry	Catalyst	Conversion, %	Yield, %
1	Fe@C-450	<1	-
2	Cu@C-450	<1	
3	Co@C-450	<1	
4	Ni@C-450	99	99
5	Ni@C-350	<1	
6	Ni@C-550	23	23
7	Ni@C-650	<1	
8	Ni@C-750	<1	
9	C-450	<1	

Reaction conditions: 0.5 mmol 1-decene, 1 bar H_2, 2 mL methanol, room temperature (25–27 °C), 8 h. 20 mg heterogeneous catalyst (8 mol % Ni). Conversion/yields were determined by GC using *n*-hexadecane as standard.

Characterizations of the Ni-Based Catalysts

To understand the structural features and reason for the excellent activity of the specific Ni@C-450 catalyst, we performed detailed characterization of this material and compared it with other less active (Ni@C-550) and inactive materials (Ni@C-350 and Ni@Al_2O_3-450). X-ray diffraction (XRD) pattern of the most active (Ni@C-450) and less active (Ni@C-550) catalysts revealed the presence of mainly metallic Ni particles, evidenced by three diffraction peaks at 44.5°, 51.8°, and 76.4° (Figures 2a and 3a).[28,29] In the inactive catalysts, Ni@C-350 and Ni@Al_2O_3-450, the presence of mainly Ni-oxide (NiO) particles is observed with the diffraction peaks at 37.2°, 43.3°, and 62.9° (Figures S1 and S2).[28,29] TEM analysis of most active (Ni@C-450) and less active (Ni@C-550) catalysts (Figures 2c and 3c) confirmed the formation of uniformly distributed metallic Ni-nanoparticles with an average diameter of 8.60 nm and 11.06 nm, respectively. Interestingly, Ni-nanoparticles in both these materials are surrounded by graphitic shells, which results in the formation of Ni NPs/graphitic shell-based core–shell struc-

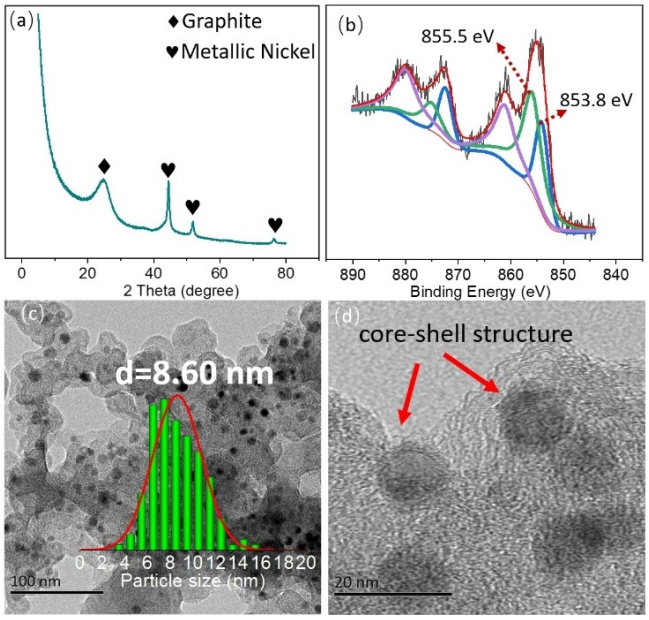

Figure 2. a) XRD pattern, b) Ni 2p XPS spectra, c) TEM images, and d) HRTEM images of Ni@C-450 catalyst. The inset of (c) shows that the particles are uniformly distributed on the carbon support with an average diameter of 8.60 nm. d) Formation of Ni NPs/graphitic shell-based core–shell structures.

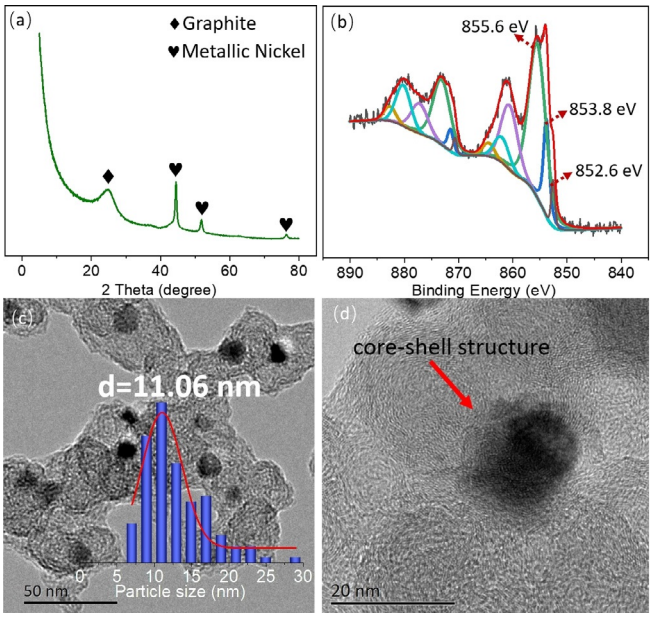

Figure 3. a) XRD pattern, b) Ni 2p XPS spectra, c) TEM images, and d) HRTEM images of Ni@C-550 catalyst. The inset of (c) shows that the particles are uniformly distributed on the carbon support with an average diameter of 11.06 nm. d) Formation of Ni NPs/graphitic shell-based core–shell structures.

tures (Figures 2d and 3d). The formation of these newly formed graphitic shells is due to the carbonization of carbon support.[30] The bigger particle size in Ni@C-550 (11.06 nm) catalyst compared to Ni@C-450 (8.60 nm) is induced by the higher calcination temperature. To know more about the nature of Ni-particles on the surface, XPS analysis was conducted. The Ni 2p spectra of four catalysts (Ni@C-450, Ni@C-350, Ni@C-550, and Ni@Al_2O_3-450) were deconvoluted into three contributions at approximately 852.5, 853.8, and 855.5 eV in the Ni $2p_{3/2}$ region, which are assigned to metallic nickel, NiO, and Ni_2O_3, respectively.[29] These data revealed only the presence of Ni-oxide particles in Ni@C-450 (Figure 2b), Ni@C-350 (Figure S4), and Ni@Al_2O_3-450 (Figure S5), while Ni@C-550 (Figure 3b) contained a mixture of Ni-oxide and metallic Ni.

The structural defects of Ni@C-350, Ni@C-450, and Ni@C-550 were analyzed using Raman spectroscopy (Figure S7). The D and G band peaks at around 1354 and 1599 cm^{-1} were observed in all these samples. The D band originated from the defected carbon and the G band is due to crystallized graphitic sp^2 carbon.[31,32] The different intensity ratios of D/G (I_D/I_G) resulted from the calcination temperatures, which affect the interaction between Ni and carbon support. As shown in Figure S7, the defect degree of Ni@C-450 is the highest ($I_D/I_G = 1.003$). As the calcination temperature rises to 550 °C, the value of I_D/I_G decreases from 1.003 to 0.992, indicating that higher calcination temperature increases the graphitization degree of the graphite layer covering nickel nanoparticles. This means the nickel nanoparticles in Ni@C-550 were more tightly wrapped by the graphitic carbon layers, which obviously hinder the contact between reactants and nickel nanoparticles; consequently its catalytic activity is much lower than that of Ni@C-450 (Table 1, entries 12 and 14). Finally, N_2 physisorption experiments were conducted to study the textural properties of the materials (Table S3, and Figures S8, S9).

As shown in Table S3, Ni@C-450 has the largest specific surface area of 204 $m^2 g^{-1}$; hence, it can provide more sites to adsorb reactants. The recycled Ni@C-450 catalyst was also analyzed by XRD, XPS, and BET. XPS showed the presence of metallic nickel particles in this sample in addition to Ni-oxide particles. This can be attributed to the reduction of some of the Ni-oxides to metallic Ni on the surface of the catalyst by hydrogen during the reaction (Figure S6). However, no significant changes for the recycled catalyst were observed compared to the fresh one by XRD (Figure S3) and BET (Figures S8 and S9).

All these characterization results revealed that the formation of monodisperse small Ni-nanoparticles and the generation of graphitic shells which surround the particles are key features for the most active catalytic material (Ni@C-450). The larger surface area and higher degree of defects of the Ni@C-450 catalyst can provide more reactive sites for adsorption and catalysis. The core–shell structure prevents metal leaching, which certainly improves stability. Due to these structural features, Ni@C-450 showed the best catalytic performance for the benchmark hydrogenation.

Hydrogenation of Aliphatic Olefins

The general applicability of Ni@C-450 was first tested in the hydrogenation of a series of aliphatic alkenes. Using the optimal Ni-catalyst, simple alkenes including terminal acyclic (**1**–**4**) and internal cyclic (**5**–**10**) moieties were hydrogenated to give the corresponding alkanes in excellent yields (Scheme 1). By prolonging the reaction time, high conversion of more sterically hindered internal cyclic alkenes (**10** and **11**) was also achieved.

Alkenes containing hydroxy and ether groups (**14**–**16**) are also selectively hydrogenated. 2-Methoxy-4-allylphenol (**18**), a renewable feedstock derived from lignin, provided 2-methoxy-4-propylphenol, which is of potential interest for polymers[33] and carbamates,[34] in 97% yield. Similarly, the more demanding 1,3,5-tribromo-2-prop-2-enoxybenzene (**19**) was hydrogenated to 1,3,5-tribromo-2-propoxybenzene in excellent yield without any reductive dehalogenation side reactions. Notably, functional groups, such as nitrile, ketone, ester, and epoxide groups, were well tolerated during the hydrogenation process as well (**21**–**27**). Finally, the natural monocyclic terpene (+)-limonene (**28**) was selectively reduced to (+)-carvomenthene by using our catalytic system.

Hydrogenation of Aromatic Alkenes

Under the previously optimized conditions, a variety of aromatic alkenes are selectively reduced, too. Styrene (**29**) and substituted derivatives bearing electron-withdrawing (**30**–**32**) and -donating groups (**33** and **34**) provided the corresponding ethyl benzenes in quantitative yields. Hydro-

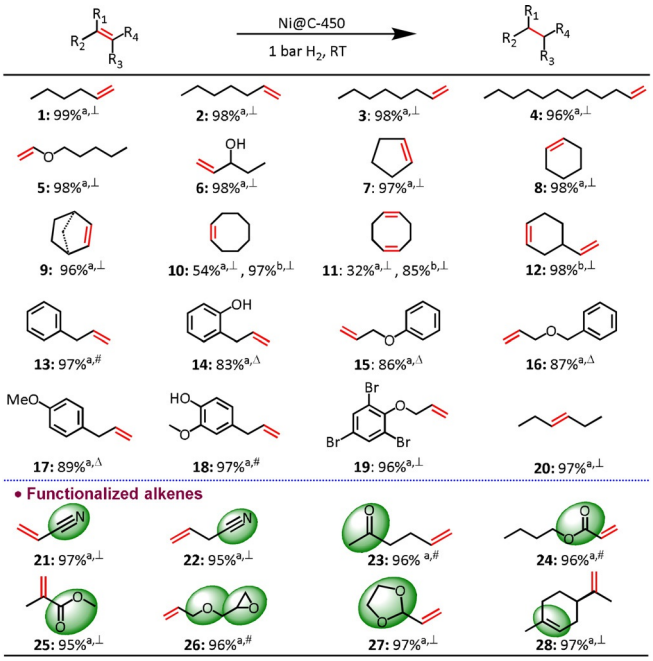

Scheme 1. Hydrogenation of aliphatic alkenes using Ni@C-450 catalyst. Reaction conditions: [a] 0.5 mmol alkene, 20 mg catalyst (8 mol% Ni), 2 mL methanol, RT, 1 bar H_2, 8 h; [b] 16 h. $^{\perp}$Yields were determined by GC using hexadecane as standard. $^{\#}$Yields were determined by ^{1}H NMR using mesitylene as internal standard. $^{\Delta}$Isolated yields.

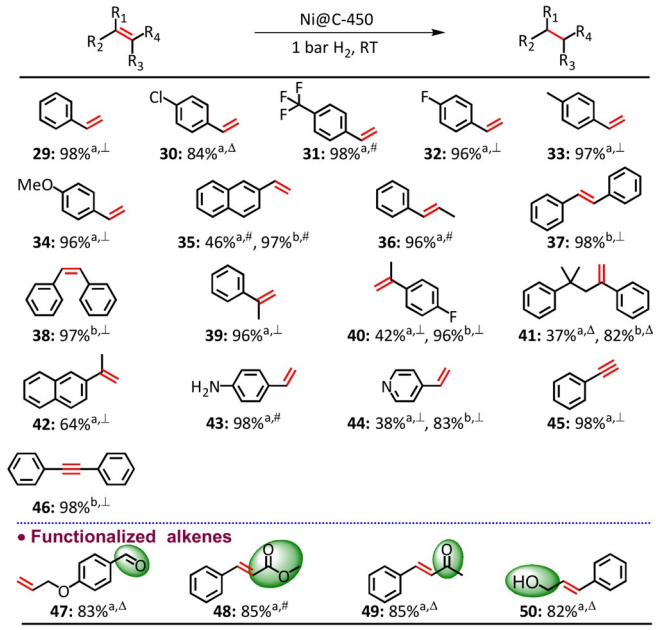

Scheme 2. Ni@C-450-catalyzed hydrogenation of aromatic alkenes. Reaction conditions: [a] 0.5 mmol substrate, 20 mg catalyst (8 mol% Ni), 2 mL methanol, RT, 1 bar H_2, 8 h; [b] 16 h. $^{\perp}$Yields were determined by GC using hexadecane as standard. $^{\#}$Yields were determined by ^{1}H NMR using mesitylene as internal standard. $^{\Delta}$Isolated yields.

genation of *trans*-stilbene (**37**) was achieved in 98% yield. In addition, the hydrogenation of 1,1-disubstituted alkenes (**39**–**42**), which is challenging for many catalysts,[7,35,36] proceeded smoothly (Scheme 2).

As an example, 2-methyl-2,4-diphenylpentane was obtained in 82% yield despite the steric hindrance of the two phenyl groups (**41**). In several cases the hydrogenation of N-heterocycles and amino-olefins is hampered by strong coordination of the nitrogen atom(s), which hinders or slows down C–C double bond reductions. Interestingly, with the present catalyst olefinic bonds in presence of these N-moieties (**43** and **44**) were reduced easily to give the corresponding alkanes in up to 85% yield. In addition to alkenes, aromatic alkynes can be completely hydrogenated. Here, both terminal and internal alkynes such as phenylacetylene (**45**) and 1,2-diphenylacetylene (**46**) were fully reduced to corresponding alkanes in 98% yield. From a synthetic perspective it is interesting that Ni@C-450 also allowed for the highly selective hydrogenation of terminal (**47**) and internal (**48**–**50**) C–C double bonds in the presence of other reducible groups such as aldehyde (**47**), ester (**48**), and ketones (**49**).

Hydrogenation of Sterically Hindered Alkenes, 1,n-Dienes, and Trienes

As shown in Table 2, diverse internal and sterically hindered alkenes can be selectively hydrogenated in good to excellent yields at comparably low temperature (45 °C). Both electron-rich and electron-poor double bonds can be hydrogenated in high yields under these conditions (compare Table 2, entries 1, 3 and 7). In case of (natural) substrates with more than one olefinic unit, in general complete hydrogenation can be achieved (Table 2, entries 2, 4, 5, 6, and 9).

Table 2: Hydrogenation of sterically hindered alkenes, 1,*n*-dienes, and trienes using Ni@C-450 catalyst.

Entry	Substrate	Product	Yield
1			2%[a], 99%[b]
2	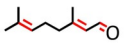		2%[a], 47%[b]
3			3%[a], 96%[b]
4	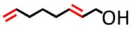	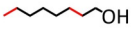	97%[a], 99%[b]
5	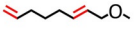	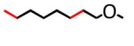	98%[a], 99%[b]
6			3%[a], 79%[b]
7			4%[a], 86%[b]
8			4%[a], 83%[b]
9			2%[a], 69%[b]

Reaction conditions: 20 mg Ni@C-450, 0.5 mmol substrate, 2 mL methanol, 16 h. [a] RT, 1 bar H_2. [b] 45 °C, 5 bar H_2. Yields were determined by GC using hexadecane as standard.

Hydrogenation of Sunflower Oil

The hydrogenation of vegetable oil is an important industrial process to produce triglycerides with higher boiling point and increased degree of saturation.[11] To showcase the applicability of the new catalyst, commercial sunflower oil consisting predominantly of unsaturated fatty acid triglycerides (89% purity) was hydrogenated at 25 bar for 18 h (Scheme 3).

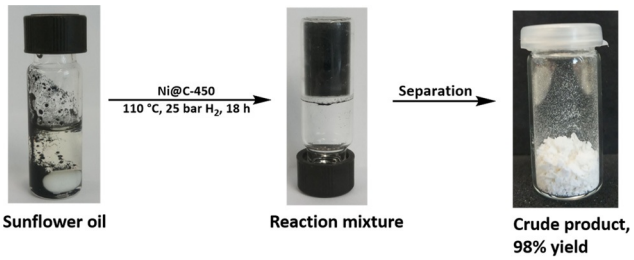

Scheme 3. Hydrogenation of sunflower oil over Ni@C-450 catalyst. Reaction conditions: 2 mL sunflower oil, 20 mg Ni@C-450 catalyst, 110 °C, 18 h, 25 bar H_2. Yield was calculated from the mass difference before and after reaction. Details of separation are presented in the Supporting Information.

Notably, in these cases no additional solvent was used. Indeed, hydrogenation took place already at 80 °C (48% conversion); however increased conversion was obtained at 110 °C. Afterwards, the reaction mixture was completely solidified. The catalyst can be easily recycled from this solid mixture by dissolving the crude product in methanol and after filtration a white solid is obtained in which 58% of the olefinic groups are hydrogenated.

Selective Deuteration of Alkenes

The performance of our Ni-based catalyst in the hydrogenation of alkenes prompted us to test its applicability also for the deuteration of alkenes using D_2 gas. Such deuterium-labeled compounds are useful probes in many mechanistic investigations, including reaction kinetics as well as for metabolic studies.[18,37–39] Gratifyingly, in presence of 1 bar of D_2 at room temperature seven alkenes were selectively converted into their corresponding labeled alkanes with excellent yields. As far as we know, this is the first example for achieving deuteration of alkenes at ambient conditions using a heterogeneous non-noble metal catalyst. Interestingly, in all cases the deuterium incorporation is higher at the terminal position (α) compared to the internal position (β), which has been also observed in mechanistic experiments of a recently disclosed iron-catalyzed transfer hydrogenation of olefins (for further mechanistic explanations, see the next section).[18]

Mechanistic Studies

To rationalize the activity of our novel catalyst system several control experiments were completed. First, we wanted to exclude the possibility of additional transfer hydrogenations in the presence of methanol, which was used in most experiments as the solvent. As shown by reactions (1) and (2) in Scheme 4, the reduced product 4-*n*-propylanisole was only

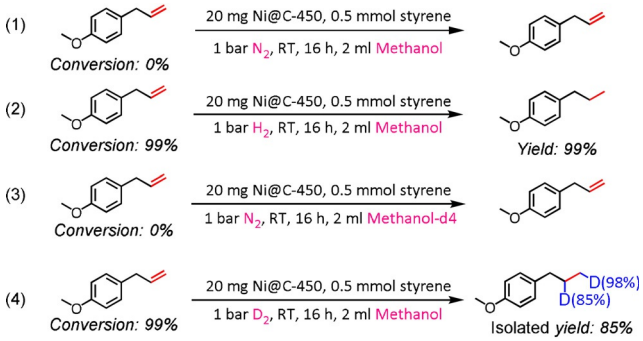

Scheme 4. Control experiments for the hydrogenation and deuteration of 4-allylanisole.

formed in the presence of molecular hydrogen. In agreement with the result from reaction (1), in the presence of $[D_4]$MeOH no deuterium-labeled product is formed (Scheme 4, reaction (3)). Notably, in deuteration studies with D_2 (Table 3 and Scheme 4, reaction (4)), apart from the deuterated alkane, MeOD was also detected by ^{2}H NMR after the reaction. We presume MeOD is formed by H/D-exchange between methanol and Ni–D species. Based on all

Table 3: Selective deuteration of alkenes to deuterium-labeled alkanes catalyzed by Ni@C-450 catalyst.

Entry	Substrate	Deuteration Percentage	Conversion	Isolated Yield
1	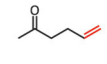	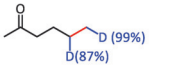 D (99%) D(87%)	>99%	78%
2	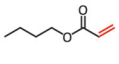	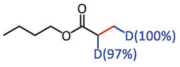 D(100%) D(97%)	>99%	81%
3	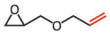	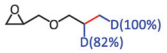 D(100%) D(82%)	>99%	79%
4		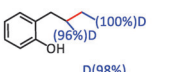 (100%)D (96%)D	>99%	83%
5	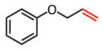	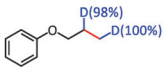 D(98%) D(100%)	>99%	86%
6	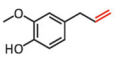	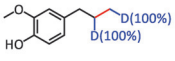 D(100%) D(100%)	>99%	80%
7	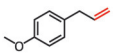	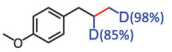 D(98%) D(85%)	>99%	85%
8	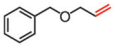	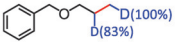 D(100%) D(83%)	>99%	84%

Reaction conditions: 0.5 mmol alkene, 20 mg catalyst, 1 bar D_2, RT, 2 mL methanol, 16 h. Conversion was determined by GC using hexadecane as standard. Deuteration percentage of α or β position was determined by comparison of ^{1}H NMR and ^{2}H NMR.

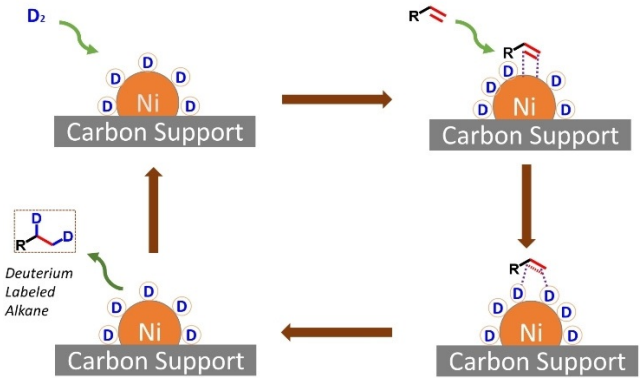

Scheme 5. Proposed mechanism for the deuteration of terminal alkenes.

these results, we propose the following plausible reaction mechanism: As shown in Scheme 5, initially, H_2 or D_2 is activated by the Ni@C-450 catalyst at room temperature, thereby leading to the formation of active Ni−H or −D species. Based on the formation of MeOD, we assume a reversible exchange between Ni−H/D and MeO−H on the catalyst surface. After adsorption on the surface of Ni@C-450, the alkene will insert into the metal−H or −D bond to provide the corresponding metal alkyl species. Since deuterium incorporation is higher at the terminal position (α) compared to the internal position (β) after reaction, we conclude a stepwise process for the formation of the new C−H/D bonds. Finally, desorption of the alkane regenerates the active catalyst material.

Catalyst Stability and Recycling

To prove the stability of this novel catalyst, several recycling experiments were performed for the benchmark reaction using different conditions. Indeed, Ni@C-450 can be reused conveniently and after six times no significant loss of catalytic activity is observed at complete and lower conversion (Figure 4). Interestingly, the separation of the catalyst is straightforward without any filtration or centrifugation by simply using a magnet.

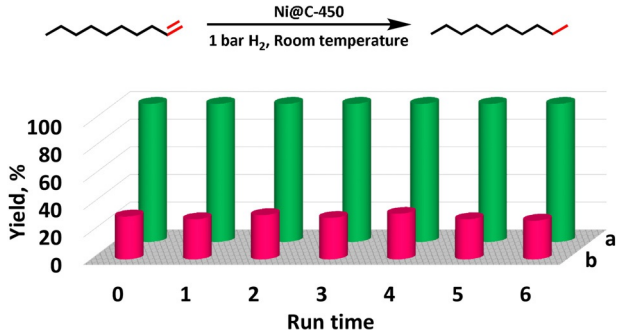

Figure 4. Recycling and stability of Ni@C-450 in the hydrogenation of 1-decene. [a] Reaction conditions for complete conversion: 0.5 mmol 1-decene, 20 mg Ni@C-450, 2 mL methanol, RT, 1 bar H_2, 8 h. [b] Reaction conditions for less than 50% conversation: same as [a] with 10 mg catalyst for 4 h.

Conclusion

Here, we describe a novel nanostructured Ni-catalyst for practical and convenient hydrogenation of various alkenes. Calcination of simple Ni-salts on carbon support creates a highly stable and reusable core–shell material, which activates hydrogen and deuterium at ambient conditions (room temperature, 1 bar). The optimal catalyst (Ni@C-450) showed excellent activity and selectivity for the hydrogenation of terminal and internal aliphatic and aromatic alkenes including functionalized ones. Noteworthy, different deuterium-labeled alkanes can be prepared using Ni@C-450 at room temperature in presence of 1 bar D_2.

Acknowledgements

We gratefully acknowledge the European Research Council (EU project 670986-NoNaCat) and the State of Mecklenburg–Vorpommern for financial and general support. Jie Gao and Rui Ma thank the China Scholarship Council (CSC) for financial support. We thank the analytical staff of Leibniz-Institut für Katalyse e.V., Germany and Dalian Institute of Chemical Physics, China for their excellent service. Open access funding enabled and organized by Projekt DEAL.

Conflict of Interest

The authors declare no conflict of interest.

Keywords: alkenes · catalysis · deuteration · hydrogenation · nanoparticles

[1] a) Y. Kissin, *Alkene Polymerization Reactions with Transition Metal Catalysts*, 1st ed., Elsevier Science, Amsterdam, **2008**; b) E. S. Cueny, M. R. Nieszala, R. D. J. Froese, C. R. Landis, *ACS Catal.* **2021**, *11*, 4301 – 4309.
[2] a) B. Morandi, Z. K. Wickens, R. H. Grubbs, *Angew. Chem. Int. Ed.* **2013**, *52*, 2944; *Angew. Chem.* **2013**, *125*, 3016; b) R. A. Fernandes, A. K. Jha, P. Kumar, *Catal. Sci. Technol.* **2020**, *10*, 7448 – 7470.
[3] a) H. C. Kolb, M. S. VanNieuwenhze, K. B. Sharpless, *Chem. Rev.* **1994**, *94*, 2483; b) G. Dong, P. Teo, Z. K. Wickens, R. H. Grubbs, *Science* **2011**, *333*, 1609.
[4] *Epoxides: Synthesis Reactions and Uses (Chemistry Research and Applications)* (Eds.: R. Reeves, Maryann Lawrence), Nova Science Publishers, Hauppauge, **2017**.
[5] T. E. Müller, K. C. Hultzsch, M. Yus, F. Foubelo, M. Tada, *Chem. Rev.* **2008**, *108*, 3795 – 3892.
[6] Y. Wang, A. Kostenko, S. Yao, M. Driess, *J. Am. Chem. Soc.* **2017**, *139*, 13499 – 13506.
[7] S. Monfette, Z. R. Turner, S. P. Semproni, P. J. Chirik, *J. Am. Chem. Soc.* **2012**, *134*, 4561 – 4564.
[8] A. Primo, F. Neatu, M. Florea, V. Parvulescu, H. Garcia, *Nat. Commun.* **2014**, *5*, 5291.

[9] R. Xu, S. Chakraborty, S. M. Bellows, H. Yuan, T. R. Cundari, W. D. Jones, *ACS Catal.* **2016**, *6*, 2127 – 2135.
[10] R. C. Cammarota, C. C. Lu, *J. Am. Chem. Soc.* **2015**, *137*, 12486 – 12489.
[11] F. K. Scharnagl, M. F. Hertrich, C. Kreyenschulte, H. Lund, R. Jackstell, M. Beller, *Sci. Adv.* **2018**, *4*, eaau1248.
[12] F. S. Mederos, J. Ancheyta, I. Elizalde, *Appl. Catal. A* **2012**, *425 – 426*, 13 – 27.
[13] B. M. Goortani, A. Gaurav, A. Deshpande, F. T. T. NG, G. L. Rempel, *Ind. Eng. Chem. Res.* **2015**, *54*, 3570 – 3581.
[14] a) G. Rubulotta, K. L. Luska, C. A. Urbina-Blanco, T. Eifert, R. Palkovits, E. A. Quadrelli, C. Thieuleux, W. Leitner, *ACS Sustainable Chem. Eng.* **2017**, *5*, 3762 – 3767; b) A. Sreenavya, A. Sahu, A. Sakthivel, *Ind. Eng. Chem. Res.* **2020**, *59*, 11979 – 11990.
[15] L. Solange, B. Sonia, M. Bernard, M. Jacqueline Luche, A. Marquet, *J. Am. Chem. Soc.* **1977**, *100*, 1558 – 1563.
[16] U. P. Laverdura, L. Rossi, F. Ferella, C. Courson, A. Zarli, R. Alhajyoussef, K. Gallucci, *ACS Omega* **2020**, *5*, 22901 – 22913.
[17] A. Pews-Davtyan, F. K. Scharnagl, M. F. Hertrich, C. Kreyenschulte, S. Bartling, H. Lund, R. Jackstell, M. Beller, *Green Chem.* **2019**, *21*, 5104 – 5112.
[18] M. Espinal-Viguri, S. E. Neale, N. T. Coles, S. A. Macgregor, R. L. Webster, *J. Am. Chem. Soc.* **2019**, *141*, 572 – 582.
[19] K. Tokmic, C. R. Markus, L. Zhu, A. R. Fout, *J. Am. Chem. Soc.* **2016**, *138*, 11907 – 11913.
[20] G. Hahn, P. Kunnas, N. de Jonge, R. Kempe, *Nat. Catal.* **2018**, *2*, 71 – 77.
[21] L. C. Liu, A. Corma, *Chem. Rev.* **2018**, *118*, 4981 – 5079.
[22] I. Yarulina, K. De Wispelaere, S. Bailleul, J. Goetze, M. Radersma, E. Abou-Hamad, I. Vollmer, M. Goesten, B. Mezari, E. J. M. Hensen, J. S. Martinez-Espin, M. Morten, S. Mitchell, J. Perez-Ramirez, U. Olsbye, B. M. Weckhuysen, V. Van Speybroeck, F. Kapteijn, J. Gascon, *Nat. Chem.* **2018**, *10*, 804 – 812.
[23] Y. Zhang, X. J. Cui, F. Shi, Y. Q. Deng, *Chem. Rev.* **2012**, *112*, 2467 – 2505.
[24] L. Zhang, Y. Ren, W. Liu, A. Wang, T. Zhang, *Natl. Sci. Rev.* **2018**, *5*, 653 – 672.
[25] R. V. Jagadeesh, K. Murugesan, A. S. Alshammari, H. Neumann, M. M. Pohl, J. Radnik, M. Beller, *Science* **2017**, *358*, 326 – 332.
[26] R. V. Jagadeesh, A. E. Surkus, H. Junge, M. M. Pohl, J. Radnik, J. Rabeah, H. Huan, V. Schünemann, A. Brückner, M. Beller, *Science* **2013**, *342*, 1073.
[27] X. Kang, H. Liu, M. Hou, X. Sun, H. Han, T. Jiang, Z. Zhang, B. Han, *Angew. Chem. Int. Ed.* **2016**, *55*, 1080; *Angew. Chem.* **2016**, *128*, 1092.
[28] Y. Zhang, X. J. Cui, F. Shi, Y. Q. Deng, *Chem. Rev.* **2012**, *112*, 2467 – 2505.
[29] J. Gao, Q. Jiang, Y. Liu, W. Liu, W. Chu, D. S. Su, *Nanoscale* **2018**, *10*, 14207 – 14219.
[30] J. Li, Y. Zhou, X. Xiao, W. Wang, N. Wang, W. Qian, W. Chu, *ACS Appl. Mater. Interfaces* **2018**, *10*, 41224 – 41236.
[31] S. Li, Y. Liu, H. Gong, K.-H. Wu, H. Ba, C. Duong-Viet, C. Jiang, C. Pham-Huu, D. Su, *ACS Appl. Nano Mater.* **2019**, *2*, 3780 – 3792.
[32] S. Li, Q. Gu, N. Cao, Q. Jiang, C. Xu, C. Jiang, C. Chen, C. Pham-Huu, Y. Liu, *J. Mater. Chem. A* **2020**, *8*, 8892 – 8902.
[33] W. Schutyser, S. Van den Bosch, J. Dijkmans, S. Turner, M. Meledina, G. Van Tendeloo, D. P. Debecker, B. F. Sels, *ChemSusChem* **2015**, *8*, 1805 – 1818.
[34] Z. Dobi, B. N. Reddy, E. Renders, L. Van Raemdonck, C. Mensch, G. De Smet, C. Chen, C. Bheeter, S. Sergeyev, W. A. Herrebout, B. U. W. Maes, *ChemSusChem* **2019**, *12*, 3103 – 3114.
[35] S. Bell, B. Wüstenberg, S. Kaiser, F. Menges, T. Netscher, A. Pfaltz, *Science* **2006**, *311*, 642.
[36] N. G. Léonard, P. J. Chirik, *ACS Catal.* **2018**, *8*, 342 – 348.
[37] T. R. Puleo, A. J. Strong, J. S. Bandar, *J. Am. Chem. Soc.* **2019**, *141*, 1467 – 1472.
[38] T. Maegawa, Y. Fujiwara, Y. Inagaki, H. Esaki, Y. Monguchi, H. Sajiki, *Angew. Chem. Int. Ed.* **2008**, *47*, 5394 – 5397; *Angew. Chem.* **2008**, *120*, 5474 – 5477.
[39] A. Di Giuseppe, R. Castarlenas, J. J. Perez-Torrente, F. J. Lahoz, V. Polo, L. A. Oro, *Angew. Chem. Int. Ed.* **2011**, *50*, 3938 – 3942; *Angew. Chem.* **2011**, *123*, 4024 – 4028.

Manuscript received: April 22, 2021
Accepted manuscript online: June 2, 2021
Version of record online: June 24, 2021

